batteries

Article

Identification and Error Analysis of Lithium-Ion Battery Oriented to Cloud Data Application Scenario

Fang Zhang [1], Tao Sun [1,*], Bowen Xu [1], Yuejiu Zheng [1,2], Xin Lai [1] and Long Zhou [1]

[1] School of Mechanical Engineering, University of Shanghai for Science and Technology, Shanghai 200093, China
[2] State Key Laboratory of Automotive Safety and Energy, Tsinghua University, Beijing 100084, China
* Correspondence: tao_sun531@163.com

Abstract: The label-less characteristics of real vehicle data make engineering modeling and capacity identification of lithium-ion batteries face great challenges. Different from ideal laboratory data, the raw data collected from vehicle driving cycles have a great adverse impact on effective modeling and capacity identification of lithium-ion batteries due to the randomness and unpredictability of vehicle driving conditions, sampling frequency, sampling resolution, data loss, and other factors. Therefore, data cleaning and optimization is processed and the capacity of a battery pack is identified subsequently in combination with the improved two-point method. The current available capacity is obtained by a Fuzzy Kalman filter optimization capacity estimation curve, making use of the charging and discharging data segments. This algorithm is integrated into a new energy big data cloud platform. The results show that the identification algorithm of capacity is applied successfully from academic to engineering fields by charge and discharge mutual verification, and that life expectancy meets the engineering requirements.

Keywords: electric vehicle; cloud data; error analysis; capacity estimation

check for updates

Citation: Zhang, F.; Sun, T.; Xu, B.; Zheng, Y.; Lai, X.; Zhou, L. Identification and Error Analysis of Lithium-Ion Battery Oriented to Cloud Data Application Scenario. *Batteries* **2023**, *9*, 216. https://doi.org/10.3390/batteries9040216

Academic Editor: Carlos Ziebert

Received: 22 October 2022
Revised: 7 January 2023
Accepted: 10 January 2023
Published: 3 April 2023

1. Introduction

Different from the laboratory-labeled data of lithium-ion batteries, the cloud data collected from vehicle driving cycles limits the possible application of multi-path battery capacity modeling to a certain extent. It is difficult to calibrate battery model parameters for vehicles in service. On the other hand, the cloud data do not have life labels. At the same time, the accuracy of the lithium-ion battery capacity model based on the accumulated charge method between two points is affected by the accuracy of state of charge (SOC) [1]. However, due to systematic and random errors in sampling, the SOC in real vehicle data cannot accurately reflect the real SOC.

Currently, there are three prevalent SOC estimation methods: the first technique directly adopts the SOC of the Battery Management System (BMS), which may be its actual estimated value or its apparent value. The former error depends on the accuracy of the developed state estimation algorithm, whereas the later error assumes that the user experience is typically a pseudo-SOC that cannot reflect the actual SOC.

The second method is to use SOC estimation based on a model-driven method [2] combined with various types of filtering [3–6]. Usually, the model needs additional test identification. For example, the first-order RC model can be used to estimate the battery SOC [7], and the second-order Randles circuit can be used to construct the state space and estimate the state variable SOC in combination with the individual impedance measured by Electrochemical Impedance Spectroscopy (EIS) [8]. The state filtering algorithm can also be optimized to estimate and update the SOC [9]. Considering that Equivalent Circuit Model (ECM) parameter identification needs to be carried out under laboratory conditions, it is difficult to schedule battery cells and calibrate parameters for cloud platform service

vehicles. In addition, ECM parameter mismatches due to differences between laboratory and real vehicle conditions may still occur even if they can be calibrated.

The third method is based on the specific relationship of OCV-SOC, which collects monomer OCV to directly map SOC. This method can ensure the accuracy of SOC under the premise of sufficient static depolarization. Considering that EV has a long resting interval, the method of Professor Sauer's team from RWTH Aachen University is conducive to directly measure SOC by collecting charged OCV based on the OCV-SOC curve mapping relationship [10]. Therefore, a charging interval screening link is added before executing the algorithm, which requires the vehicle to have a certain rest period before charging. In addition, considering the effect of temperature on battery capacity, the temperature should be relatively constant during charging. Therefore, a relatively accurate capacity analysis based on the accumulated electricity between two points can only be triggered if the above two conditions are met. However, in practical engineering, there are few user behaviors that can meet the requirements of charging after resting, and users are generally used to charging after resting or discharging after resting. Therefore, data fragments satisfying the requirements of resting are less in the charging part and more in the discharging part, and the static premise accurately mapped by OCV-SOC is available in the discharging part.

Aiming at improving the accuracy of SOC estimation, the systematic and random errors are analyzed in the collection of real vehicle cloud data based on real vehicle unlabeled data and combine the improved accumulated power between two points method to solve the available capacity. Moreover, the correction strategy of on-vehicle SOC is analyzed to obtain a more reliable SOC acquisition method. Finally, the Kalman filter with fuzzy logic is introduced to optimize the robustness of the model. Through the above steps, the capacity identification model of a lithium-ion battery under cloud big data scenario is obtained and verified.

The content of this paper is organized as follows: Section 2 analyzes the two-point method. Section 3 analyzes the systematic error and random error of real vehicle cloud signal sampling and proposes the optimization method. Section 4 proposes an adaptive filter based on fuzzy logic to improve the accuracy of the results. Section 5 presents the results and verification of the proposed methods. Section 6 summarizes the proposed methods and prospects for future work.

2. Improved Two-Point Method for Engineering Application

The two-point method is a commonly method used to calculate battery capacity [11–14]. This method can be applied in the laboratory, but it is difficult to use in vehicle driving cycles [15]. Therefore, this section adopts other methods based on partial charging curves to improve the two-point method. This paper defines the capacity as the ratio of battery charging and discharging ampere hours to the difference between SOC before and after [16], and derives the following Formula (1):

$$\mathrm{SOC}(t_2) = \mathrm{SOC}(t_1) + \frac{1}{C}\int_{t_1}^{t_2} \frac{CEi(t)}{3600} dt \tag{1}$$

where $\mathrm{SOC}(t_2)$ is the state of charge of the battery at time t_2, $\mathrm{SOC}(t_1)$ is the state of charge of the battery at time t_1, C is the total capacity of the battery cell in ampere hours, and $i(t)$ is the current in ampere at time t. CE is the coulomb efficiency. $CE \approx 1$ because the side reaction rate of lithium-ion batteries is relatively low compared with lead-acid or nickel hydrogen batteries [17]. The integral operation is performed in seconds and converted into hours. It is specified that the current $i(t)$ at the time of discharge is negative and the charging current is positive, and the following Formula is derived (2):

$$C = \frac{\int_{t_1}^{t_2} \frac{CEi(t)}{3600} dt}{\mathrm{SOC}(t_2) - \mathrm{SOC}(t_1)} \tag{2}$$

According to Formula (2), the accuracy of battery capacity calculation depends on both the integration accuracy of charge and discharge current and the SOC calculation accuracy.

The estimation accuracy of SOC may be related to the evaluation rate and resolution of cloud collection and the SOC correction strategy of vehicle end in actual projects. The error of SOC will be analyzed and optimization methods will be proposed later.

3. Error Analysis

The data in this paper are provided by a company. Taking some key parameters as potential errors in an engineering application that may be encountered in sampling and calculation, this section divides all errors into nonrandom systematic errors, including sampling frequency and sampling resolution; and random errors, including electricity integration error, charging interval, temperature change, and SOC correction strategy; combined with actual cases to carry out analysis and algorithm optimization.

3.1. System Errors Originated from Sampling Frequency and Resolution

The system error is repetitive, which is generally inherent in the system itself. The sampling frequency and parameter sampling resolution of cloud data are usually determined during the platform construction. Different frequencies and resolutions will affect the capacity estimation as system errors.

The sampling frequency determines the amount of data. High-frequency sampling will get more specific data but also increase the burden of platform storage. Therefore, frequency division sampling technology is proposed to cope with the load and fidelity of electric vehicle (EV) cloud data upload. The event-driven method can be used to sample only when the signal value changes, to reduce the memory requirements of low-frequency signals on a large scale. For high-frequency data, the high-frequency signals can be discarded by fast Fourier transform combined with trial-and-error method, and the optimal storage frequency can be determined by inverse Fourier transform.

The sampling resolution of the battery signal will also cause capacity calculation error. Some key parameters and resolution are shown in Table 1. The resolution basically meets the requirements of the national standard. Among them, the SOC sampling step size is 1%, which may cause capacity estimation error. Therefore, analysis should be carried out and corresponding algorithm optimization should be designed.

Table 1. Sampling resolution.

Parameter	Resolution Ratio
Time	year-month-day-hour-minute-second
Mileage	kilometers
Voltage	0.1 V
Current	0.1 A
SOC	1%
Temperature	1 °C

Figure 1 shows the SOC and quantity (Q) diagram calculated from the cloud charging data of an electric vehicle. The sampling resolution of SOC is 1%. Take charging $\Delta SOC = 2\%$ as an example and take the traditional accumulated electricity between two points for analysis; its current capacity should be the slope value of the blue dashed line in Figure 1 that is, $\Delta Q/\Delta SOC$. However, because the SOC resolution is only 1%, the metering points are stacked. In fact, if the SOC sampling resolution is sufficient, the real SOC-Q points should be distributed like red dots. Although the collected data corresponding to 86% SOC is unreliable, the first SOC-Q point triggered to 87% SOC is relatively reliable, and the subsequent points cannot be guaranteed because the actual SOC should be between 87~88%, and the actual capacity after optimization should be the slope of the red dashed line in the figure.

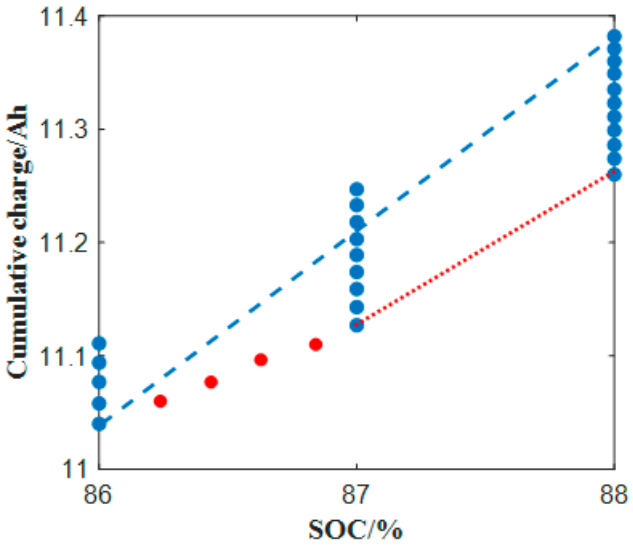

Figure 1. SOC Resolution optimization strategy.

3.2. Random Errors Originated from Coulometric Integration and Charging Segment

In addition to the system error that may be caused by the inherent sampling frequency and resolution of the cloud platform itself, uncertain random factors such as current or time jump, temperature change, and the SOC correction strategy set by the manufacturer in the calculation process will also constitute random errors for cloud capacity identification. This section will analyze the possible random errors in combination with cases and optimize the algorithm to reduce the random errors of capacity cloud identification.

During the charging and discharging process of electric vehicles, potential dynamic errors or data packet loss accompany the battery signal sensors and data uploading, resulting in the transient jump of current and the data vacancy of time segments. To improve it, choose a more stable current segment to calculate the metering integration, and make a differential observation on the time series. If the time jump is too large, the electricity integration will be significantly affected.

The interval and length of the charging SOC captured by the accumulated charge between two points will also affect the capacity estimation. By constructing the charging SOC transformation matrix to observe the influence of different charging starting SOCs on the fluctuation of capacity life calculation, it can be found that the longer the SOC interval, the more stable and reliable the identified capacity life will be. In engineering practice, the reason why SOC calculated under low SOC and high SOC is feasible is that the battery changes rapidly with OCV in the low SOC interval, as shown in Figure 2. The SOC correction strategy carried by the current general BMS adopts the method driven by amp-hour integration fusion model to carry out fast correction in this interval. Based on the above correction principle of SOC in engineering practice, the charging and discharging interval segments that meet the initial conditions of SOC can be directly screened to optimize the random error influence of charging interval on capacity calculation.

3.3. SOC Correction Strategy

In engineering, to give users a better experience, engineers usually add a modification strategy to the actual SOC. This section will analyze various potential correction strategies combined with real cloud data to minimize the capacity estimation error caused by SOC correction strategies.

In the low SOC interval, the linearity of the OCV-SOC curve is high, as shown in Figure 3. The SOC changes rapidly with the OCV. It is believed that the SOC algorithm carried by the general BMS will use the method of fusion model filtering to carry out faster correction in this interval. The SOC at this time should be a relatively reliable SOC after filtering and fusion correction value.

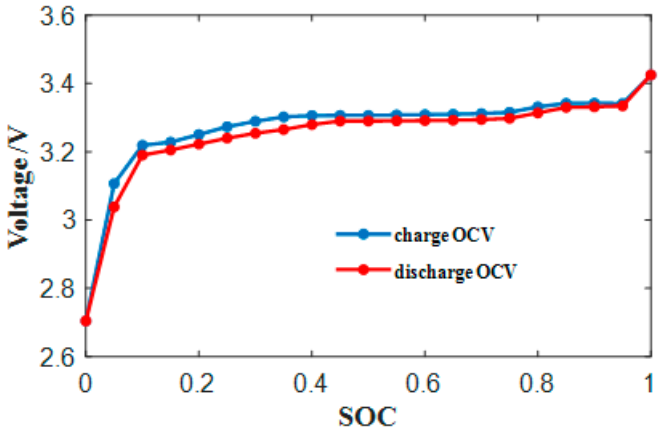

Figure 2. OCV-SOC Characteristic curve.

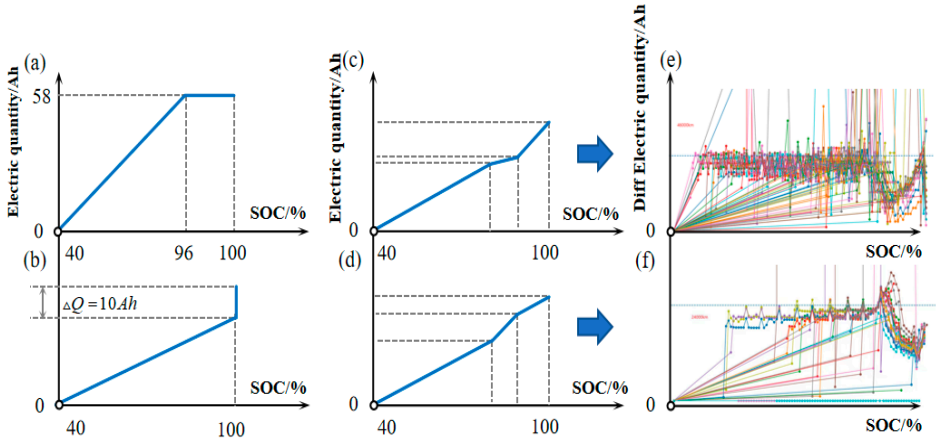

Figure 3. High SOC correction strategy (**a**–**f**).

There is also a correction problem in the high SOC interval [18]. A typical correction of the upper cut-off voltage corresponding to 100% SOC is shown in Figure 3a,b. The former corresponds to a small apparent SOC estimate, and the latter corresponds to a large apparent SOC estimate. In Figure 3a, the SOC of the display will reach 100% soon after the charge reaches 96%. The SOC of the display is smaller than the actual state. When the actual state of the battery has reached the upper cut-off voltage, the SOC of the display will be corrected to 100% immediately because the estimation error is still 96%. In Figure 3b, when the charging reaches 100% SOC, the charging state is not ended immediately. From this, the apparent SOC is larger than the actual one. When the apparent SOC reaches 100%, the actual state of the battery has not reached the upper cut-off voltage, and the charging is completed after it reaches it. The core of the above two kinds of correction strategies is that the true state of charge of the battery must correspond to 100% when the upper cut-off voltage is reached; before the cut-off voltage is reached, the SOC presented is not reliable, and there is a large or small cumulative error.

In addition to the above cut-off voltage correction, there is also dynamic correction as shown in Figure 3c,d in the high SOC section. In the actual charging data sampling, the correction phenomenon as shown in Figure 3e,f is also captured, which correspondingly verifies the actual existence of the correction strategy as shown in Figure 3c,d. With regard to online capacity cloud identification based on charging segments, it is the most reliable SOC_{min}, which should be as low as 30% SOC. For the SOC_{max}, it should correspond to the upper cut-off voltage or the high SOC interval of more than 95% shall be selected as far as possible. The SOC intercepted meeting these two conditions is relatively reliable for capacity identification of the accumulated electricity between two points.

In addition, SOC can also be corrected after standing. Before EV startup, BMS can map SoC based on OCV by looking up the table. By studying the relationship between voltage change and standing time, it is required that the standing time should meet 3 h. Considering the user's charging and discharging behavior, there are few charging segments in the cloud data of the real vehicle that meet the requirements of 3 h standing, but in the discharge process, there are many segments that meet the requirements of 3 h standing. Therefore, when the OCV-SOC correction strategy is oriented to practical applications, it is easier to meet the static requirements in the discharge section.

3.4. Temperature Correction

As one of the most important parameters, battery temperature affects battery power, durability, and safety [1]. Lithium-ion activity is also different at different temperatures, and the temperature difference leads to fluctuations in the available capacity of the battery, resulting in random errors in capacity estimation at different temperatures [19]. According to the temperature performance test of the battery, the discharge capacity of the battery in the low-temperature environment decreased significantly, and the discharge capacity in the high-temperature environment increased slightly. As shown in Figure 4, the relationship between temperature and depth of discharge (DOD) shows that the lithium battery is fully discharged at 25 °C. Therefore, when modeling the capacity of lithium-ion batteries in the cloud-oriented big data scenario, it is necessary to uniformly correct the capacity at different temperatures to 25 °C. Based on empirical formulas, the identification results can be corrected by the following formula (3):

$$Cap_{std} = Cap_i \times (1 - 0.02 \times (T_{ave} - 25) \div 10) \quad (3)$$

where Cap_{std} is the standard capacity after temperature correction, and T_{ave} is the average temperature of the temperature measuring point.

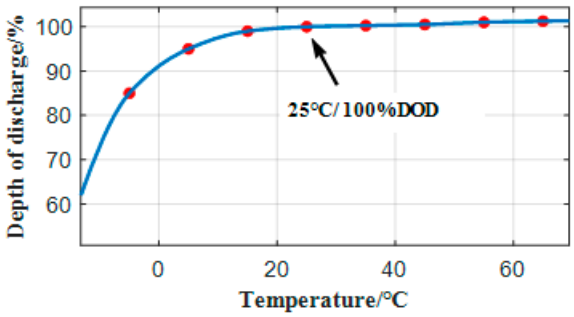

Figure 4. Temperature-DOD.

4. Adaptive Filtering Based on Fuzzy Logic Rules

Due to the inherent system and random errors of real vehicle cloud data, the capacity identification results tend to fluctuate and diverge. In this section, a filter correction algorithm [20] will be designed based on the preliminary identification of capacity, and the observation noise in the state space will be adjusted in real time according to different SOC of charge/discharge start/end in combination with fuzzy logic (FL) to calculate a more reasonable and accurate capacity estimation result.

Specifically, after the preliminary capacity values are obtained based on the charge and discharge segments, the final capacity estimation results are obtained by Kalman filter (KF) optimization of fuzzy noise control. When establishing the state space of the filtering system, considering the slow attenuation of the battery capacity, it is considered that the capacity is basically the same before and after the time, and there is some system noise ω_i. The state space of the battery capacity is:

$$x_{i+1} = x_i + \omega_i \quad (4)$$

$$y_i = x_i + v_i \tag{5}$$

where x_i, as capacity, considers the small attenuation of charge and discharge capacity and the system noise ω_i. The smaller value meets the filtering requirements. y_i is used to output the observed values of the equation, considering the influence of different charging intervals on the estimation accuracy $v_i = e^{\alpha} v_0$. Variable observation noise is used, α is determined by fuzzy logic according to the charging start and end states, and v_0 is the general observation noise constant.

The flow of determining the variable observation noise value based on fuzzy logic is shown in Figure 5, $C_T(i)$ by i capacity observations of the sequence, combined with the sequence $i-1$. Capacity estimation results of $C_E(i-1)$. The capacity estimation result is obtained after KF optimization controlled by fuzzy logic $C_E(i)$. Continue to participate in the state filtering of the next time series, form a closed-loop correction, and iteratively estimate the real system capacity state. The main basis for formulating fuzzy rules is: $\mathrm{SOC_{min}}$, and relative error e_Q. Smaller output α Value; $\mathrm{SOC_{max}} \geq 99\%$. Configure small observation noise V_i.

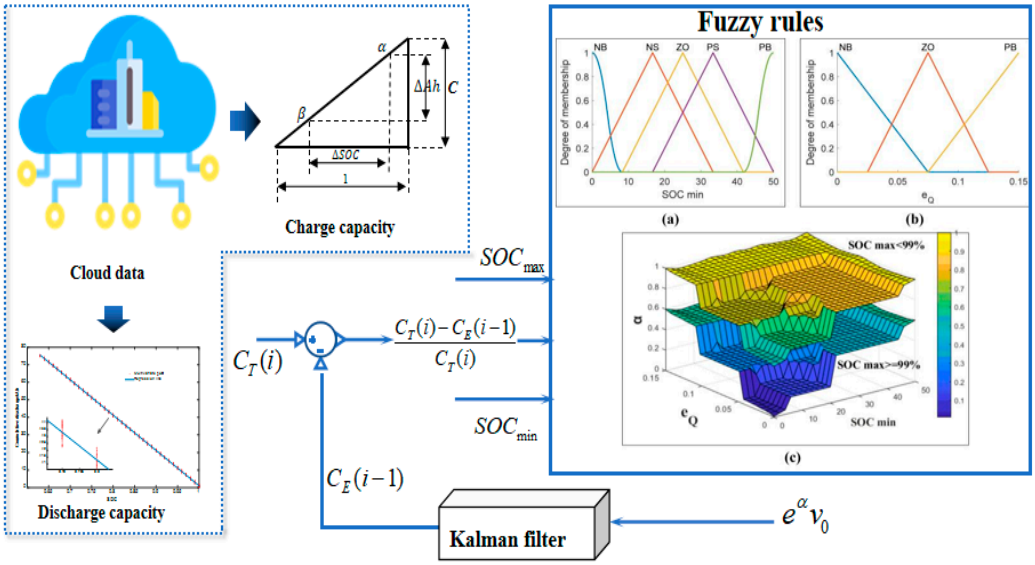

Figure 5. FL + KF flow chart.

5. Results and Discussion

Based on the principle of accumulated electricity between the above two points and the analysis of the systematic and random errors in the data of the cloud platform of real vehicles, this section will study the capacity identification algorithm based on the two-point method and the multi-point method in combination with the charging segment and the discharging segment based on the actual operation data of 100 real vehicles, and use the Kalman filter of fuzzy logic to evaluate and analyze the current available capacity life of the battery system.

5.1. Identification of Charging Segment Capacity

By analyzing the correction strategy of the charging SOC in the random error, the charging segments that meet a certain interval are strictly screened. It is required that the starting SOC of the charging segment should be less than 30%, and the SOC at the end of the charging should be the corresponding SOC when the upper cut-off voltage is reached, or the high SOC interval of more than 95%.

Figure 6 shows the capacity life of the battery system identified in this study based on the collected cloud charging data of 100 vehicles, where each color represents the identified capacity of a vehicle based on the charging data within two months, and a single circle represents the capacity identified based on a single charge. The error fluctuation of single

capacity estimation is due to the inherent system error and random error, but it does not affect the overall trend of attenuation. It is worth noting that about three of the 100 vehicles may have premature capacity aging due to multi-layer consistency and potential faults, as shown in the filled circle in Figure 5. It is necessary to carry out return inspection in combination with enterprises.

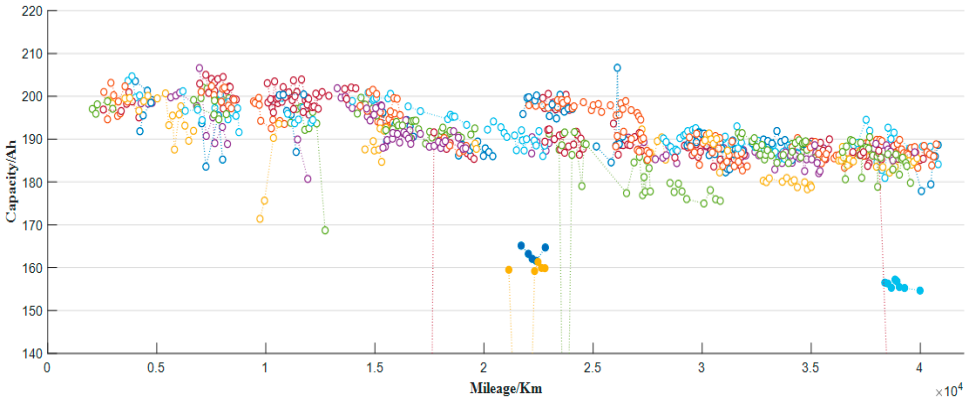

Figure 6. Charging capacity estimation results.

5.2. Identification of Discharging Segment Capacity

Compared with the SOC reliability of the charging segment, the discharging segment can theoretically measure more accurate SOC. Compared with the user's charging habits, the discharge segment is more likely to meet the long-term standing segment, so it can be corrected by using the OCV-SOC look-up table to obtain more accurate SOC.

For the system capacity identification of discharge segments, this section applies the method of multi-point linear regression to optimize the original two-point cumulative electricity method. The SOC calculation formula at the discharge stage is as follows in Equation (6):

$$\mathrm{SOC}(t_i) = \frac{Q(t_i)}{C} = \frac{Q(t_0) - \int_{t_0}^{t_i} I(t)dt}{C} \tag{6}$$

wherein $Q(t_i)$ by t_i. The multiple linear regression form of the remaining power at any time obtained by transformation is shown in Formula (7):

$$\int_{t_0}^{t_i} I(t)dt = Q(t_0) - C \times \mathrm{SOC}(t_i) \tag{7}$$

$Q(t_0)$ and capacity C are unknown; accumulated discharge $\int_{t_0}^{t_1} I(t)dt$ is known. The accumulated error in the discharge segments that meet the screening conditions has been eliminated, so the $\mathrm{SOC}(t_i)$ is accurate to a certain extent. Define a multi-point representation as $\left(\int_{t_0}^{t_1} I(t)dt, \mathrm{SOC}(t_i)\right)$; therefore, the $\int_{t_0}^{t_1} I(t)dt$ and $\mathrm{SOC}(t_i)$ linear relationship between can be reflected by multi-point regression as shown in Figure 7.

Therefore, the current available capacity of the battery for the discharge segment can be identified by Equation (8) through linear regression. For convenience of expression, let $qi = \int_{t_0}^{t_i} I(t)dt$.

$$C = \frac{\sum_{i=0}^{n} q_i \sum_{i=0}^{n} \mathrm{SOC}(t_i) - n \sum_{i=0}^{n} qi\mathrm{SOC}(t_i)}{n \sum_{i=0}^{n} \mathrm{SOC}(t_i)^2 - \left(\sum_{i=0}^{n} \mathrm{SOC}(t_i)\right)^2} \tag{8}$$

Figure 8 shows the capacity life of the battery system identified in this study based on the cloud discharge data of real vehicles. Compared with the number of available charging segments, due to the continuity of the long discharge interval, more segments can meet the screening requirements, and the attenuation trend consistent with the charging calculation results and individual vehicles with premature capacity aging can also be observed.

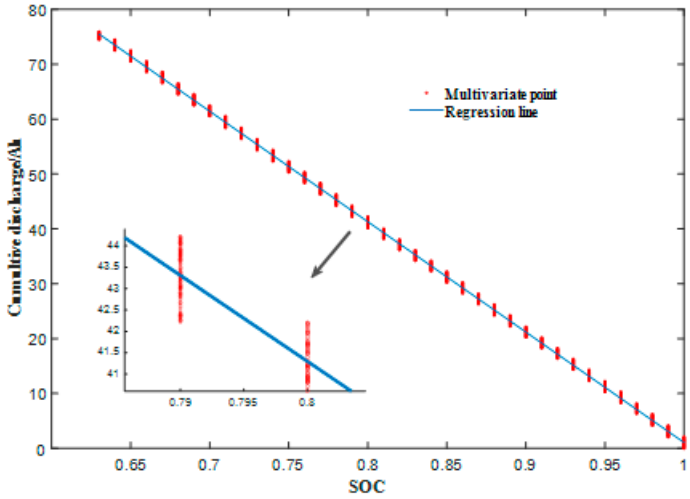

Figure 7. Multiple point linear regression.

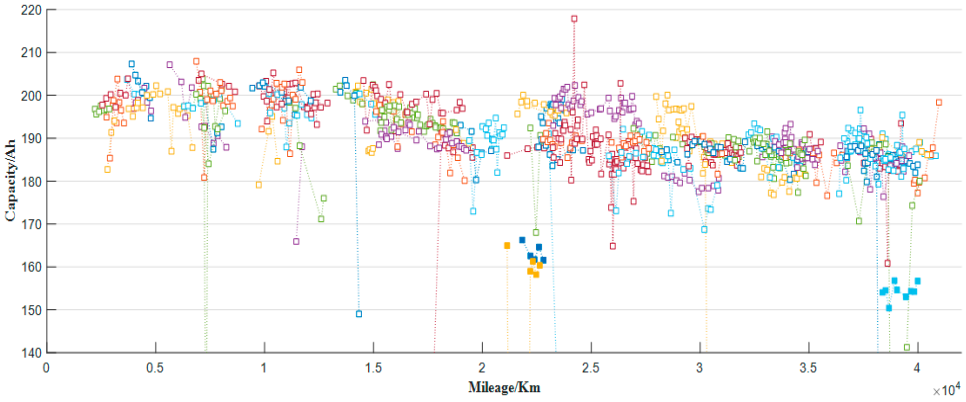

Figure 8. Estimation of discharge capacity of 100 real vehicles.

5.3. Fuzzy Kalman Identification of Charge and Discharge Capacity

The real system capacity state after filtering is shown in Figure 9. The Kalman filter based on fuzzy logic can reasonably and effectively remove the system state noise, and the trend conforms to the attenuation law of lithium-ion batteries. Among them, circles and boxes are the identification results of charge and discharge capacity, respectively, which are basically the same.

Figure 9. FL + KF capacity estimation result.

The algorithm verifies the capacity from the perspective of charging and discharging data segments. According to the attenuation evolution, the system capacity of this model decays from 200 ah to about 185 ah in the range of 0–40,000 km, and can travel to about 110,000 km if the retirement boundary is 80%. In fact, most users will not choose to retire, so the reasonable mileage life is expected to reach 200,000 km. If users drive 60 km a day, the battery life can reach about 9 years.

The real-time life estimation algorithm developed in this study is integrated into the new energy big data monitoring cloud platform in Sichuan, as shown in Figure 10, which realizes the application of the algorithm from academic to engineering fields.

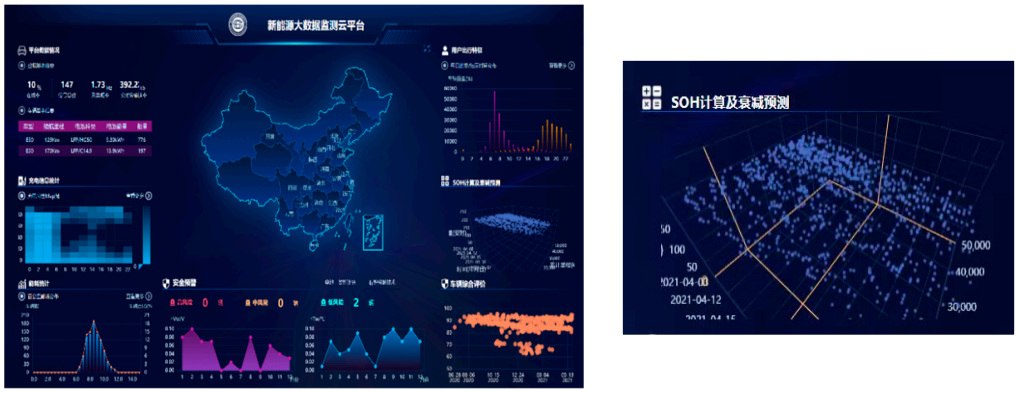

Figure 10. UI interface of big data monitoring cloud platform of Sichuan new energy innovation center.

6. Conclusions

To reflect real capacity changes, the lithium-ion battery capacity estimation model is established by the raw data of vehicle driving cycles on the cloud. First, the causes of capacity estimation issues are analyzed using the accumulated charge method between two points. Then, using real vehicle data that has been sampled from the cloud, the systematic and random mistakes in cloud sampling are analyzed. A correction method is then presented and developed for accurately determining the real SOC of the system, as well as the range between high and low SOC. The fuzzy logic Kalman filter optimizes the capacity estimation curve. Finally, using the charging and discharging data segments, the battery system's current available capacity is determined. The capacity identification curve derived from the established capacity estimation model of a lithium-ion battery is in accordance with the decay trend of the battery system, as confirmed by the cloud data of 100 real vehicles of a vehicle enterprise, and the mileage life of the modified model is anticipated to reach 200,000 km. The algorithm has also been implemented into a company's big data detection cloud platform, and the estimation accuracy has passed the platform's verification, accomplishing the algorithm's transition from academic to engineering stages.

In the subsequent study, based on this research, the current research group will predict the capacity based on the capacity estimation and precisely forecast the battery service period.

Author Contributions: T.S.: Methodology, Data curation, Writing—review and editing. F.Z.: Software, Data curation, Validation, Writing—original draft. B.X.: Data curation, Writing—review and editing. Y.Z.: Supervision, Writing—review and editing. X.L.: Supervision, Writing—review and editing. L.Z.: experimental instruction, Writing—review and editing. All authors have read and agreed to the published version of the manuscript.

Funding: This research is supported by Natural Science Foundation of Shanghai under the Grant number of 23ZR1444600, in part by the National Natural Science Foundation of China (NSFC) under the Grant number of 52277222.

Acknowledgments: The authors thank the National Natural Science Foundation of China (NSFC) under the Grant number of 52277222, Natural Science Foundation of Shanghai under the Grant number of 23ZR1444600. Furthermore, thank you to Tao Sun, Bowen Xu, Yuejiu Zheng, Xin Lai, and Long Zhou for support in the realization of the test and the method.

Conflicts of Interest: The authors declare no conflict of interest.

Abbreviations

The following abbreviations are used in this manuscript:

SOC	State of charge
ECM	Equivalent circuit model
EIS	Electrochemical Impedance Spectroscopy
OCV	Open circuit voltage
EV	Electric Vehicle
Q	Quantity
DOD	Depth of discharge
FL	Fuzzy logic
KF	Kalman filter
BMS	Battery Management System

References

1. Su, L.; Wu, M.; Li, Z.; Zhang, J. Cycle life prediction of lithium-ion batteries based on data-driven methods. *Etransportation* **2021**, *10*, 100137. [CrossRef]
2. Sepasi, S.; Ghorbani, R.; Liaw, B.Y. Inline state of health estimation of lithium-ion batteries using state of charge calculation. *J. Power Sources* **2015**, *299*, 246–254. [CrossRef]
3. Sun, J.; Tang, C.; Li, X.; Wang, T.; Jiang, T.; Tang, Y.; Chen, S.; Qiu, S.; Zhu, C. A remaining charging electric quantity based pack available capacity optimization method considering aging inconsistency. *Etransportation* **2022**, *11*, 100149. [CrossRef]
4. Shen, P.; Ouyang, M.; Lu, L.; Li, J.; Feng, X. The Co-estimation of State of Charge, State of Health, and State of Function for Lithium-Ion Batteries in Electric Vehicles. *IEEE Trans. Veh. Technol.* **2018**, *67*, 92–103. [CrossRef]
5. Guo, Y.; Zhao, Z.; Huang, L. SoC Estimation of Lithium Battery Based on AEKF Algorithm. In Proceedings of the 8th International Conference on Applied Energy (ICAE), Beijing Institute Technology, Beijing, China, 8–11 October 2017.
6. Wang, J.; Zhang, Z. Lithium-ion Battery SOC Estimation Based on Weighted Adaptive Recursive Extended Kalman Filter Joint Algorithm. In Proceedings of the 8th IEEE International Conference on Computer Science and Network Technology (ICCSNT), Dalian, China, 20–22 November 2020; IEEE: New York, NY, USA; pp. 11–15.
7. Li, X.; Yuan, C.; Wang, Z.; He, J.; Yu, S. Lithium battery state-of-health estimation and remaining useful lifetime prediction based on non-parametric aging model and particle filter algorithm. *Etransportation* **2022**, *11*, 100156. [CrossRef]
8. Einhorn, M.; Conte, F.V.; Kral, C.; Fleig, J. A Method for Online Capacity Estimation of Lithium Ion Battery Cells Using the State of Charge and the Transferred Charge. *IEEE Trans. Ind. Appl.* **2012**, *48*, 736–741. [CrossRef]
9. Zhou, X.; Pan, Z. An online capacity estimation method for lithium ion battery cells using the significant points. In Proceedings of the 43rd Annual Conference of the IEEE-Industrial-Electronics-Society (IECON), Beijing, China, 29 October–1 November 2017; IEEE: New York, NY, USA; pp. 2750–2754.
10. Farmann, A.; Waag, W.; Marongiu, A.; Sauer, D.U. Critical review of on-board capacity estimation techniques for lithium-ion batteries in electric and hybrid electric vehicles. *J. Power Sources* **2015**, *281*, 114–130. [CrossRef]
11. Song, Z.; Yang, X.-G.; Yang, N.; Delgado, F.P.; Hofmann, H.; Sun, J. A study of cell-to-cell variation of capacity in parallel-connected lithium-ion battery cells. *Etransportation* **2021**, *7*, 100091. [CrossRef]
12. Sun, T.; Jiang, S.; Li, X.; Cui, Y.; Lai, X.; Wang, X.; Ma, Y.; Zheng, Y. A Novel Capacity Estimation Approach for Lithium-Ion Batteries Combining Three-Parameter Capacity Fade Model with Constant Current Charging Curves. *IEEE Trans. Energy Convers.* **2021**, *36*, 2574–2584. [CrossRef]
13. Sun, T.; Wang, S.; Jiang, S.; Xu, B.; Han, X.; Lai, X.; Zheng, Y. A cloud-edge collaborative strategy for capacity prognostic of lithium-ion batteries based on dynamic weight allocation and machine learning. *Energy* **2022**, *239*, 122185. [CrossRef]
14. Sun, T.; Xu, B.; Cui, Y.; Feng, X.; Han, X.; Zheng, Y. A sequential capacity estimation for the lithium-ion batteries combining incremental capacity curve and discrete Arrhenius fading model. *J. Power Sources* **2021**, *484*, 229248. [CrossRef]
15. Jian, L.; Yongqiang, Z.; Larsen, G.N.S.; Snartum, A. Implications of road transport electrification: A long-term scenario-dependent analysis in China. *Etransportation* **2020**, *6*, 100072. [CrossRef]
16. Plett, G.L. Recursive approximate weighted total least squares estimation of battery cell total capacity. *J. Power Sources* **2011**, *196*, 2319–2331. [CrossRef]

17. Liu, G.; Lu, L.; Li, J.; Ouyang, M. Thermal Modeling of a LiFePO4/Graphite Battery and Research on the Influence of Battery Temperature Rise on EV Driving Range Estimation. In Proceedings of the 9th IEEE Vehicle Power and Propulsion Conference (VPPC), Beijing, China, 15–18 October 2013; IEEE: New York, NY, USA; pp. 370–374.
18. López-Ibarra, J.A.; Goitia-Zabaleta, N.; Herrera, V.I.; Gaztañaga, H.; Camblong, H. Battery aging conscious intelligent energy management strategy and sensitivity analysis of the critical factors for plug-in hybrid electric buses. *Etransportation* **2020**, *5*, 100061. [CrossRef]
19. You, H.; Zhu, J.; Wang, X.; Jiang, B.; Sun, H.; Liu, X.; Wei, X.; Han, G.; Ding, S.; Yu, H.; et al. Nonlinear health evaluation for lithium-ion battery within full-lifespan. *J. Energy Chem.* **2022**, *72*, 333–341. [CrossRef]
20. Yang, H.; Wang, P.; An, Y.; Shi, C.; Sun, X.; Wang, K.; Zhang, X.; Wei, T.; Ma, Y. Remaining useful life prediction based on denoising technique and deep neural network for lithium-ion capacitors. *Etransportation* **2020**, *5*, 100078. [CrossRef]